

THE X-RAY HALO OF NOVA V1974 CYGNI (NOVA CYGNI 1992) AND THE NATURE OF INTERSTELLAR DUST

JOHN S. MATHIS AND DAVID COHEN

Department of Astronomy, University of Wisconsin, 475 N. Charter St., Madison, WI 53706;
 mathis, cohen@madraf.astro.wisc.edu

JOHN P. FINLEY

Department of Physics, 1396 Physics Building, Purdue University, West Lafayette, IN 47907-1396; finley@purds1.physics.purdue.edu

AND

J. KRAUTTER

Landessternwarte, Königstuhl, D-69117 Heidelberg, Germany; jkrautte@hp2.lsw.uni-heidelberg.de

Received 1994 November 7; accepted 1995 February 17

ABSTRACT

Nova V1974 Cygni (Nova Cygni 1992) was observed by *ROSAT* as a very bright soft X-ray source, with its point source image surrounded by an extensive halo caused by scattering from interstellar grains. We have analyzed the halo of 1992 December 6, using the standard extinction law ($R = 3.1$) as an additional constraint on the size distribution of the grains. We considered composite grains (with silicates and amorphous or hydrogenated carbon intermixed), possibly containing vacuum within the grains. We also included small graphite grains to provide the $\lambda 2175$ bump.

A critical parameter is the interstellar extinction between us and the nova. We estimate the reddening $E(B-V)$ to be in the range 0.19–0.31 mag, with the low reddening suggested by the $H\alpha/H\beta$ ratio as determined at the Pine Bluff Observatory. For these reddenings, composite grains can provide a good fit to both the X-ray halo and optical/ultraviolet extinction, provided that the fraction of vacuum is $\geq 25\%$ for the larger grains in the distribution ($a \geq 0.1 \mu\text{m}$). If $E(B-V) = 0.3$, as suggested by the $\text{He II } \lambda 4686/\lambda 1640$ ratio, the fit is slightly worse than for low reddening. The difficulty in fitting is providing enough extinction per H atom in the optical without producing too strong a halo. *The halo of Nova Cygni 1992 suggests that interstellar grains contain a substantial fraction of vacuum.* Probably the greatest uncertainty in this conclusion arises from the calculation of the optical properties of the composite grains.

We cannot fit the observations with all types of carbon. Hydrogenated amorphous carbon and (to a lesser extent) “organic refractory” material fail to provide enough optical extinction and the proper slope to the X-ray halo. Every reasonable model has a maximum in the mass distribution $a^4 n(a)$ (the mass per interval of $\log a$) at $a \approx 0.15\text{--}0.3 \mu\text{m}$, with the size increasing with the fraction of vacuum. Neither the halo nor the extinction law is a suitable diagnostic for the numbers of small grains ($a < 0.02 \mu\text{m}$).

The timing delays of the X-rays from Nova Cygni 1992 are too short (a few days) to be suitable for being a second diagnostic of the size distribution.

Subject headings: dust, extinction — novae, cataclysmic variables — stars: individual (Nova V1974 Cygni) — X-rays: stars

1. INTRODUCTION

The outburst of V1974 Cygni (Nova Cygni 1992) was discovered on 1992 February 19.1 and reached its maximum brightness of $V = 4.4$ on February 24.17. Its early bolometric and spectral evolution have been discussed by Shore et al. (1993, 1994) using the *International Ultraviolet Explorer (IUE)* and the Goddard High Resolution Spectrograph aboard the *Hubble Space Telescope*. The nova was detected by the *ROSAT* satellite on April 22 (Krautter, Ögelman, & Starrfield 1992). It became the brightest soft X-ray source in the sky as the expanding shell became more transparent to X-rays.

Scattering of X-rays by interstellar grains (Martin 1970; Mauche & Gorenstein 1986; Mathis & Lee 1991) produces a halo surrounding a point source image. The strength and shape of the halo provides an integral over the grain size distribution, weighted toward relative large grains as compared to other diagnostics of grain size distributions. This paper will deal with the constraints the nova provided on the grain size

distribution along the line of sight to the nova, while taking into account the known extinction properties of the interstellar medium (ISM) and also cosmic abundance constraints.

Another integral over the grain size distribution is provided by the average extinction law for the diffuse ISM (see, e.g., Tielens & Allamandola 1989 or Mathis 1990, 1993 for reviews). The extinction law varies in a systematic way over the entire interval $0.8 \mu\text{m}^{-1} \leq 1/\lambda \leq 10 \mu\text{m}^{-1}$ (Cardelli, Clayton, & Mathis 1989). The extinction cross section of a grain of a given size, shape, and material can be calculated from electromagnetic theory, so the interstellar extinction at each wavelength provides an integral of the size distribution over all sizes.

Other information regarding the size distribution of grains comes from the near-infrared (NIR) emission, both in the “unidentified infrared bands” and continuum. This emission arises from the transient heating of grains following the absorption of individual energetic ultraviolet (UV) photons (see Puget & Léger 1989; Désert, Boulanger, & Puget 1990 for reviews).

2. MODELING THE X-RAY SCATTERING AND OPTICAL EXTINCTION OF NOVA CYGNI 1992

2.1. Scattering: General Considerations

The radiative transfer of the X-ray halo surrounding a point source, especially if the halo is dominated by single scattering, is quite simple because the scattering angles are very small (arcminutes), rather than the wide-angle scattering that occurs in optical reflection nebulae. Since both the scattered and unscattered X-ray photons traverse almost the same paths through space, they each suffer about the same interstellar extinction, and their ratio is independent of the extinction.

At each energy, the extent of the halo is determined by an integral of the total X-ray flux (the attenuated direct flux plus previously scattered radiation) times cross sections that depend upon the density and size of the grains. Multiple scattering greatly complicates the analysis for optically thick lines of sight (Mathis & Lee 1991), but Nova Cygni 1992 (hereafter, NC92) has a small optical depth for interstellar grains (see below), and we can use the single-scattering approximation with confidence. The determination of $F_X(E)$, the nova flux arriving at the Earth at energy E , is discussed in the next section; here we consider the calculation of the halo if $F_X(E)$ is known.

We will assume that the grains are spherical, although this is not an essential restriction (Mathis & Lee 1991). Then the single-scattered intensity of the halo at angular distance θ from the source, $I^{(1)}(\theta)$, integrated over an observed bandpass of energies, is given by (Mauche & Gorenstein 1986; Mathis & Lee 1991)

$$I^{(1)} =$$

$$F_X N_H C_1 \int dE S(E) \int da a^6 n(a) \int dx f(x) (1-x)^{-2} \Phi^2(u), \quad (1)$$

where $F_X = \int F_X(E) dE$ over the bandpass; N_H is the column density of interstellar hydrogen along the line of sight (i.e., excluding the hydrogen within the nova shell); $n(a)da$ is the number of interstellar grains per H atom with radii in the interval $(a, a + da)$; $S(E)dE$ is the fraction of the flux in the energy interval $(E, E + dE)$. The variable x is the distance of the scattering grain from us, relative to the distance of the nova, and $f(x)$ is the relative density of grains at position x , normalized so that $\int f(x) dx = 1$. Usually we consider a uniform grain distribution, so that $f(x) = 1$. The function $\Phi(u)$ is the "form factor" (Bohren & Huffman 1983) that includes the assumption that the grains are spherical:

$$u = 2\pi a \theta E / [hc(1-x)], \quad (2)$$

$$= 0.147(a/0.1 \mu\text{m})[\theta(\text{arcmin})][E(\text{keV})]; \quad (3)$$

$$\Phi(u) = 3(\sin u - u \cos u)/u^3. \quad (4)$$

We see that the integral over x is dependent upon E and a , through $u(x, a, E, \theta)$. The function $\Phi^2(u)$ drops very fast at large u , as equation (4) shows, so that scattering occurs only at small angles. The constant C_1 in equation (1) is given by

$$C_1 = (1.1 \text{ cm}^2 \text{ sr}^{-1}) \left(\frac{2Z}{M} \right)^2 \left[\frac{F(E)}{Z} \right]^2 \left[\frac{\rho(\text{grain})}{\text{g m cm}^{-3}} \right]^2. \quad (5)$$

The function $F(E)/Z$, the atomic scattering factor (Henke 1981), is essentially unity because our energies of interest are not close to absorption edges of abundant elements. Equation

(5) overestimates the scattering of the grain if individual grains are opaque to the X-rays. For solid silicate grains of $a = 0.1 \mu\text{m}$, this condition occurs for energies below about 200 eV (see Fig. 1 in Martin & Rouleau 1990); for solid graphite, below 100 eV. The X-ray opacity falls roughly as E^{-2} , so for the energies that we will consider here, about 400 eV (see below), non-porous grains of radii of $0.4 \mu\text{m}$ should meet the optically thin restriction. Our models have negligible abundances of these or larger grains. Fluffy grains will have a lower opacity than the same-sized solid grain.

2.2. The X-Ray Properties of the Nova

The present paper uses a 2240 s integration taken on 1992 December 6, 291 days after outburst, providing 6.62×10^4 counts, or an average count rate of 29.54 ± 0.22 counts s^{-1} . By contrast, stellar binary sources of the same energy distribution, with $\langle kT \rangle \leq 30\text{--}40$ eV (the "supersoft" sources; see Hasinger 1994) show $\lesssim 1$ count s^{-1} , with the brightest in the sky, AG Dra, showing ≈ 8 count s^{-1} .

Figure 1 shows the *ROSAT* position sensitive proportional counter (PSPC; Pfeffermann et al. 1986) response, in counts arcmin^{-2} , as a function of angular offset from the center of the nova. The points give the average response within concentric rings $5''$ wide. The point source response is shown by the solid line; the background plus the point source is the dotted line. The halo is, obviously, very well determined. Table 1 gives the strength of the halo at various angular offsets from the center of the image.

The PSPC provides a pulse height spectrum response, $R(E)$, in various bins of nominal energy E' . This response is a convolution of the true spectrum of the source at the Earth, $F(E)$, with the known instrumental response function, $G(E, E')$:

$$R(E') = \int F(E) G(E, E') dE. \quad (6)$$

The incident flux, $F(E)$, is estimated by assuming its spectral distribution, performing the integration in equation (6), and

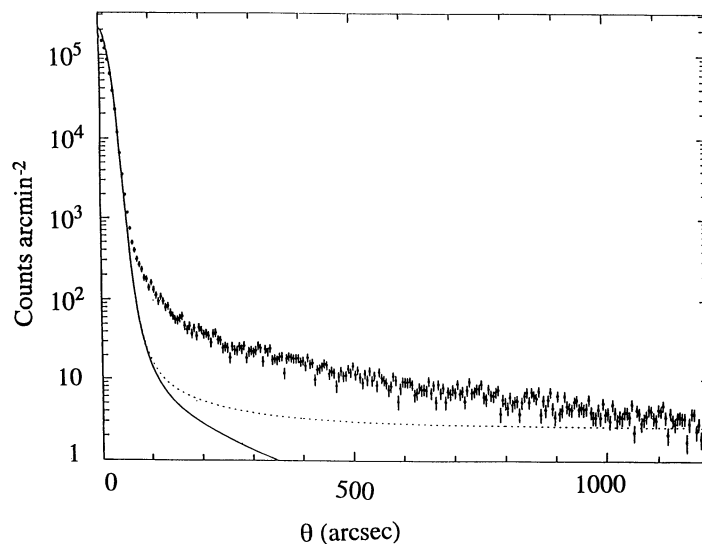


FIG. 1.—The angle-averaged PSPC counts arcmin^{-2} plotted as a function of the angular offset θ from the center of the image. The solid line is the point spread function; the dotted line is the sum of the point spread and the background. The points are the counts in annuli of $5''$ width, with the uncertainties set by photon statistics shown as error bars.

TABLE 1
STRENGTHS OF THE HALO AT VARIOUS OFFSETS
(Point source flux = 6.62×10^4 counts)

θ	$I(\text{halo})$ (counts arcmin $^{-2}$)
100''	136 ± 15
200	34 ± 4
300	17 ± 2.5
400	13.4 ± 2.0
500	8.7 ± 1.2
600	5.5 ± 1.2
800	2.4 ± 0.8

comparing the calculated response $R(E')$ to the observed one. The assumed form of $F(E)$ is based on a model that involves various parameters, which are then adjusted to achieve the best agreement of the calculated $R(E')$ with the observations. If the best fit is close to the observed $R(E')$, the assumed form for the flux must be reasonably close to the correct one.

Our adopted $F(E)$ is plotted in Figure 2a against energy, E . It produces the solid line in Figure 2b when convolved with the *ROSAT* response function. The model for $F(E)$ is a simple blackbody with a temperature $T = 2.56 \times 10^5$ K, or $kT = 0.0220$ keV, absorbed by a solar-composition gas with a hydrogen column density $N_{\text{fit}}(\text{H}) = 4.25 \times 10^{21}$ H cm $^{-2}$. The peak of blackbody photon emission occurs at $E = 2.82$ keV, or $kT = 0.0621$ keV in our model. While a blackbody is not an accurate model for the precise emission from a hot white dwarf, and our parameters would give a luminosity greatly exceeding the Eddington luminosity (Krautter et al. 1994), the actual maximum emission from the nova must be at a similar energy. The absorption by the ISM and nova shell drops dramatically with increasing energy (roughly as E^{-3}). Thus, the intervening absorption by mainly He removes almost all of the radiation below the carbon edge at 0.288 keV (the slight discontinuity in the spectrum shown in Fig. 2a), while the emission from the source is dropping rapidly towards higher energies. The spectrum received at the Earth, then, is the rather narrow region of energies, peaked at about 0.4 keV, where there is some emission and not too much absorption. Other models besides the simple blackbody with absorption were assumed for the flux of the nova at the Earth. No other intrinsic flux distribution came close to providing the observed response.

The PSPC pulse height spectrum from NC92, $R(E')$, is shown in Figure 2b, plotted against E' , the energies of the various PSPC bins. The observations of the point source of the nova are the plotted points, with error bars indicating the uncertainty caused by photon statistics alone. The solid line is for the model shown in Figure 2a. One can see that the fit of the model to the observations is very good, better than other uncertainties we will encounter in the analysis (e.g., the estimation of the scattering cross section for a grain of a given size and composition). However, there are real deviations from the simple model; see Hauschildt et al. (1994) for a discussion of the intrinsic flux of the nova source.

The Morrison & McCammon (1983) opacities, used in our work, assume a solar abundance. Actually, most of the absorption of the X-rays from the central star takes place within the nova shell rather than the ISM (see below), and the nova gas is enriched in some heavy elements (N, O, Ne, and He). These compositional differences are not crucial to our analysis; most of the opacity in both the ISM and in the nova gas would be

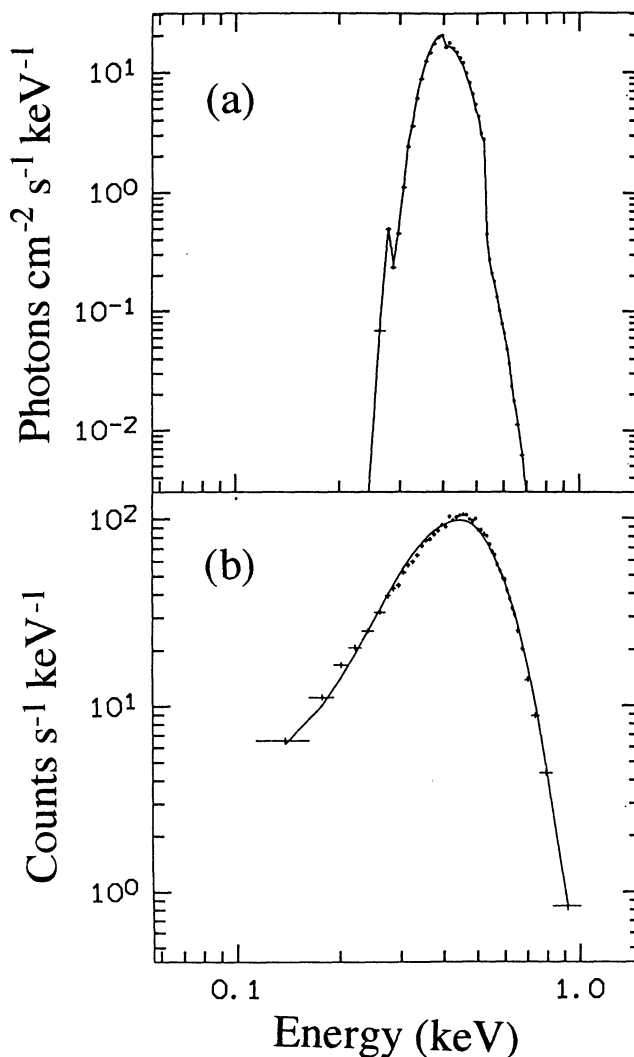


FIG. 2.—(a) The fit to the Nova Cygni 1992 spectrum of 1992 December 6 of a single blackbody model, absorbed by intervening material of cosmic composition with column density $N(\text{H}) = 4.25 \times 10^{21}$ H nuclei cm $^{-2}$, plotted against energy. The discontinuity represents the onset of additional absorption at the carbon edge, 0.288 keV. The cutoff at low energy is caused by absorption from H and He. (b) The PSPC response to the spectrum shown in (a), above. Points: the actual PSPC observation; solid line, the model shown in (a). The abscissa is the channel energy, in 10 eV bins.

provided by He, and the absorption edges of the heavier elements occur at higher energies where there is little or no flux. We regard $N_{\text{fit}}(\text{H})$ as merely a formal parameter and determine the column density of H in the ISM from ratios of emission lines originating from the nova shell. Recall that we are concerned only with comparing the observed intensity of the halo to the point-source flux at the Earth, so the excellence of the fit of the model (the correspondence of the line to the points in Fig. 1) is all that we require for analyzing the halo.

Since the scattering is always at small angles, only the grains at distances of at least hundreds of parsecs from the nova will contribute to the halo; closer grains would have to scatter through too large an angle. To analyze the halo, we must estimate the column density of interstellar dust.

We can use the Balmer decrement of the nova in its late stages to help estimate the interstellar reddening and, therefore, the column density of interstellar H in units of 10^{21} cm $^{-2}$,

$N_{21}(\text{H})$. The equivalent reddening is given by Bohlen, Savage, & Drake (1978); $E(B-V) = N_{21}(\text{H})/5.8$. Since $N_{21}(\text{H})$ is a very important parameter for determining the fluffiness of grains, we will present our results for a range of its possible values.

2.3. Fitting the X-Ray Observations and Extinction

Our approach is to assume a rather general functional form for the interstellar grain size distribution, involving several parameters. We will vary the parameters to fit the extinction for the diffuse ISM ($R = 3.1$) with the extinction law of Cardelli et al. (1989), as supplemented by O'Donnell (1994). These extinction laws are almost identical to those of Seaton (1979) or Savage & Mathis (1979). We consider wavelengths ranging from the NIR ($1 \mu\text{m}$) through the optical and UV. Of course, we will also fit the strength and shape of the X-ray halo around NC92.

We will require that the size distribution be continuous, unlike that of Mathis, Rumpl, & Nordsieck (1977, MRN), which is abruptly truncated at both large and small sizes. The smallest size we consider is $0.005 \mu\text{m}$ in radius. A proper consideration of the complete size distribution would involve a careful modeling of the very small grains or large molecules that are transiently heated by the absorption of a single photon. Their subsequent emission is observed as the "Unidentified Infrared Bands" in the $3.3\text{--}12 \mu\text{m}$ region, along with an associated continuum possibly contributing significantly to the emission out to $60 \mu\text{m}$ or even longer. These small grains contribute practically no X-ray scattering, which is the focus of the present paper. Our size distributions do not require all of the cosmic carbon or silicon, so they allow enough mass to accommodate the transiently heated grains as modeled by several authors (e.g., Draine & Anderson 1985; Puget & Léger 1989; Siebenmorgen & Krügel 1993).

Our size distribution is assumed to be

$$\ln n(a) = \ln C_2 - [p_0 + p_1 a + p_2 a^2 + p_-(0.005 \mu\text{m}/a)] \ln a, \quad (7)$$

where p_0 , p_1 , and p_2 are constants to be adjusted in the least-squares sense (see below) for the best fit to observations for various assumed values of p_- , and C_2 is determined by fitting the overall amounts of optical/UV extinction (but not X-ray scattering) per interstellar H atom. Cosmic abundance constraints also place an upper limit on C_2 .

Unlike MRN and Draine & Lee (1984), the grains are assumed to contain amorphous or possibly hydrogenated carbon, silicates, and vacuum, all mixed within the same grain (Mathis & Whiffen 1989). In addition to the composite grains, small graphite grains are assumed to be present in order to produce the 2175 \AA feature. The assumed composition of silicates are rather provisional because very recent studies of interstellar depletions (Sofia, Cardelli, & Savage 1994) show that when grains are partially destroyed the Si is released into the interstellar gas phase before Fe and Mg, indicating that the latter elements, and Si as well, are substantially combined into oxides (or some other material) rather than completely into silicates.

We feel that interstellar grains are likely to be composite, as opposed to separate silicate and graphite, because dust must circulate between dense clouds and diffuse gas on rather rapid timescales (perhaps $\approx 10^7$ yr). In the outer parts of molecular clouds the values of R often differ from the diffuse value of $R \approx 3.1$, and the extinction laws, and therefore the grain size

distributions, are different. The most reasonable interpretation of the observations is that small grains coagulate when dust enters the outer parts of dense clouds from the diffuse ISM, and large grains must shatter when moving from dense into diffuse regions. This efficient and probably rapid coagulation and shattering presumably results in the mixing of materials within the same grain, probably leaving a fraction of the grain volumes as vacuum or voids.

We do not consider silicates surrounded by large mantles of "organic refractories" (Greenberg 1989). No calculations based on these models have been presented which suggest how dust can cycle between $R = 3$ and $R \approx 4\text{--}5$. It seems difficult to see how the continuous change of the extinction law with R , unknown at the time these models were formulated, can easily be explained because there is not enough gas-phase material to provide anywhere near the required change of size of the mantles.

The determination of the optical properties of composite grains is not simple. We use the "effective medium" theory, in which the composite material is replaced by a homogeneous material whose optical properties mimic those of the composite. These theories have been discussed by Bohren & Huffman (1983) and Ossenkopf (1991). We will consider results derived from two rather different means of estimating the effective index of refraction of the composite: (a) the "Bruggeman rule" and (b) the "Maxwell-Garnett theory." Both are explained in Bohren & Huffman (1983).

There are many references giving the optical properties of "amorphous carbon" (AMC), reflecting the fact that the words denote a variety of materials whose physical properties depend upon the method of preparation and the history of annealing. Some materials are very well structured and, therefore, quite graphitic (well-ordered) in nature; others are poorly ordered, resembling soot. We considered several such materials. References to their optical properties are given in Table 2.

Rouleau & Martin (1991, hereafter RM) performed a careful analysis of laboratory absorption data (Bussoletti et al. 1987) of AMC prepared in various ways. The absorption alone is not enough to determine the real and imaginary parts of the index of refraction; RM used the Kramers-Kronig relations to provide another integral relating the real and imaginary parts of the index of refraction. The shapes of the grains enter the Kramers-Kronig relations, and RM considered several possibilities. The AMC designated "AC" by RM and in Table 2 was produced by discharge between carbon electrodes; that called "BE" is soot from burning benzene in air. RM provided two other sets of optical constants, with different grain geometries assumed, that produce results virtually identical to those of the "BE" carbon. The optical constants of Edoh in Table 2 refer to "glassy" carbon, with comparatively small domains in which the C atoms possess a regular structure. These constants

TABLE 2

REFERENCES FOR OPTICAL CONSTANTS

Material	Reference
Silicates	Draine & Lee 1984
"BE" AMC	Rouleau & Martin 1991
"AC" AMC	Rouleau & Martin 1991
HAC5, HAC9	Alterovitz et al. 1991
Edoh	Hanner 1988
"Organic refractory"	Jenniskens 1993

are plotted against energy in RM, along with their other AMC values.

The AMC constants we considered fall into only two basic types: the "AC" is rather transparent throughout the optical region, meaning that it has a relatively small imaginary part of the index of refraction, while others types from RM, and also from Etoh, are quite absorbing. We will mainly represent the high-absorption AMC constants by the model labeled "BE" in RM.

There is also good evidence that at least some, and possibly all, of the carbon in space has been hydrogenated (see Witt et al. 1989; Duley 1994). We used two sets of constants for hydrogenated amorphous carbon (HAC) from Alterovitz et al. (1991); "HAC5" contains a molar fraction of H of 12%, and "HAC9" contains 25%. The increasing molar fraction makes the HAC more transparent in the optical and near-UV.

Another possibility for carbonaceous material is "organic refractory" residues produced from processing ices by cosmic rays and UV radiation. Jenniskens (1993) has published the optical constants of this material.

We fitted a model of the size distribution of grains to observations by choosing the type of carbon from Table 2 and the parameters $E(B-V)$, p_- , and f_{vac} (the fraction of vacuum within the composite grains). The type of carbon and f_{vac} determine the grain cross sections for each size. With the cross sections we computed the optical/UV extinction per 10^{21} H atoms and the X-ray halo for various values of p_0 , p_1 , and p_2 , which collectively completely determine the grain size distribution. For each grain size distribution we minimized a χ^2 statistic (see below) by adjusting α , the mass fraction of carbon and silicates in composite grains, and β , the mass fraction of cosmic carbon in small graphite grains (needed to produce the 2175 Å bump). We assumed that small graphite had a prolate shape, as described in Mathis & Whiffen (1989), merely to shift the maximum of the extinction to 2175 Å, rather than 2110 Å for small spheres with the Draine & Lee (1984) optical constants. By adjusting α and β we minimized a χ^2 expression consisting of two parts:

$$\chi^2 = \sum_{\text{opt,UV}} \omega(\lambda) \{1 - [(\alpha\tau_{\text{model}}(\lambda) + \beta\tau_{\text{sm}}(\lambda))/\tau_{\text{obs}}(\lambda)]^2\} + \sum_{\text{X-rays}} \omega(\theta) [1 - \alpha N_{21}(\text{H}) I_{\text{calc}}^{(1)}(\theta)/I_{\text{obs}}(\theta)]^2. \quad (8)$$

The first sum in χ^2 is weighted over 10 optical/UV wavelengths, in which the extinction optical depths per 10^{21} H atoms of the model, $\tau_{\text{model}}(\lambda)$, are compared to those observed in the diffuse ISM ($R = 3.1$). The grain cross sections per 10^{21} H atoms were computed by Mie theory, with one of the effective-medium rules (Bruggeman or Maxwell-Garnett) providing the effective optical constants. The observed optical depth per H atom at each wavelength, $\tau_{\text{obs}}(\lambda)$, is known because $\tau(\lambda)/\tau(V) = A(\lambda)/A(V)$, given by Cardelli et al. (1989) and O'Donnell (1994) for the diffuse ISM. Observations (Bohlin et al. 1978) show that $E(B-V) = 0.172$ per 10^{21} H atoms, and $\tau(V) = 3.1 E(B-V)/1.086 = 0.492$.

We considered wavelengths from 1 μm to 0.125 μm . Each was assigned a weight, $w(\lambda)$ in equation (8), which was a parameter of the model. We chose to use unit weights for all wavelengths, except $w(0.2175 \mu\text{m}) = 3$.

The second sum in χ^2 contains the deviations of the single-scattering X-ray halo intensities calculated from the model, $I_{\text{calc}}^{(1)}(\theta)$, relative to the observed intensities, $I_{\text{obs}}(\theta)$, listed in Table 1. The intensities at 100" and 200" were given 5 times the

weight of the others in order to give heavy weight to the central value of the halo and to its derivative.

Almost all models minimized χ^2 with $\alpha + \beta < 1$, meaning that we do not need all of the available carbon and silicate in our model. This is fortunate because recent studies of interstellar depletions (Lacy et al. 1994; Sofia et al. 1994) show that a substantial amount of C, some 20%, is in the gas phase and not incorporated into grains. However, various determinations of the cosmic C/H ratio for young objects (see Peimbert, Torres-Peimbert, & Dufour 1994 for a recent discussion of nebular and stellar abundances) range from 10^6 C/H = 160 (B stars) to 540 (M17). Clearly, variations of $\pm 20\%$ are well within the uncertainties of the true ISM abundance (if, indeed, that quantity has any meaning in more than simply an average sense.)

If a model required $\alpha + \beta > 1$ to minimize χ^2 , we recomputed α with the condition $\beta = 1 - \alpha$.

3. RESULTS

The parameters which most affect our results are (a) the column density of interstellar hydrogen, $N_{21}(\text{H})$, or equivalently the interstellar reddening $E(B-V)$, (b) the type of carbon assumed; and (c) the fraction of vacuum assumed in the grains. We also investigated the sensitivity of our results to the uncertainties in fitting the intrinsic X-ray spectrum of the nova, the type of mixing rule used in the analysis, the relative distribution of the weights of the various optical/UV wavelengths, the value of p_- , which controls the small-grain size cutoff (see eq. [7]), and the uniformity of the distribution of the grains along the line of sight.

3.1. The Interstellar Hydrogen Column Density

The interstellar reddening, $E(B-V)$, has been estimated by a number of authors. Table 3 summarizes the various estimates.

Professor J. S. Gallagher kindly estimated the He II $\lambda 4686$ line flux on 1992 October 19 (day 240), measured with the 0.9 m telescope at the Pine Bluff Observatory (PBO) of the University of Wisconsin (Barger et al. 1993). The He II line is blended with N III $\lambda 4640$ and [Ne IV] $\lambda 4720$. The estimated flux of $\lambda 4686$, $(1.4 \pm 0.5) \times 10^{-11}$ ergs $\text{cm}^{-2} \text{s}^{-1}$, can be compared to the $\lambda 1640$ intensity, 3.0×10^{-11} ergs $\text{cm}^{-2} \text{s}^{-1}$, obtained with the IUE (SWP 46064) 1992 October 26. The ratio of the emission coefficients of $\lambda 4686$ and $\lambda 1640$ for a nebula optically thick to He II resonance transitions ("case B") is almost independent of density or temperature (Robbins 1968). The He II lines are not strong and so are not subject to serious uncertainties because of optical depth effects within the lines. The $\lambda 4686/\lambda 1640$ ratio indicates an optical depth difference, $\tau(1640) - \tau(4686)$, of 1.2 ± 0.3 . With the mean extinction law

TABLE 3
ESTIMATES FOR $E(B-V)$ FOR NOVA CYGNI 1992

$E(B-V)$	Reference
0.20 ± 0.05	Shore et al. 1994 LMC 1990
0.19.....	Balmer decrement, Barger et al. 1993, day 450, $R = 3.1$
0.3.....	Austin et al. in preparation, quoted in Hauschildt et al. 1994
0.32 ± 0.01	Chochol et al. 1993
0.35.....	This paper, He II $\lambda 4686/\lambda 1640$, $R = 3.2$
0.29.....	This paper, He II, $R = 3.4$
0.42.....	This paper, He II, $R = 3.0$
0.31.....	This paper, adopted "large" reddening

appropriate to the diffuse ISM (Cardelli et al. 1989; O'Donnell 1994), $R = 3.1$, this optical depth difference implies $A(V) = 1.0 \pm 0.3$ mag, or $E(B-V) = A(V)/R = 0.31 \pm 0.08$. Since $N_{21}(\text{H}) = 5.8 E(B-V)$ in the diffuse ISM (Bohlin et al. 1978), $N_{21}(\text{H}) = 1.8 \pm 0.4$. The uncertainty in R is at least ± 0.2 , and the typical deviations of the extinction for a specific line of sight from the mean extinction law are ± 0.2 for $\tau(1640)/\tau(V)$ (see Fig. 4 in Cardelli et al. 1989). We estimate that $E(B-V) = 0.31 \pm 0.09$ based upon the $\lambda 4686/\lambda 1640$ ratio alone.

A lower value of $E(B-V)$ is suggested by the measurement of $\log(\text{H}\alpha/\text{H}\beta)$ (Barger et al. 1993) of the nova shell on day 450, the last day as measured at the PBO. For that time $\log(\text{H}\alpha/\text{H}\beta)$ was 0.54, apparently declining in time as the shell became optically thin in the Balmer lines. A reasonable extrapolation might lead to $\log(\text{H}\alpha/\text{H}\beta) \approx 0.52$. The nova shell has, presumably, a high electron temperature ($\geq 15,000$ K) because (a) its central white dwarf ionizing source is very hot, and (b) the electron density is so high ($n_e \geq 10^6 \text{ cm}^{-3}$) that many forbidden lines are collisionally deexcited. For $T_e = 17,000$ K the ratio of the intrinsic emissivities of $\text{H}\alpha/\text{H}\beta \approx 2.75$, slightly lower than for cooler plasmas. The PBO measurement corresponds to $E(B-V) = 0.19$ if the ISM along the line of sight has $R = 3.1$. Any $[\text{N II}] \lambda 6548, 6583$ present in the spectrum would be blended with $\text{H}\alpha$, leading to an overestimate of the reddening and a decrease of the true $E(B-V)$. However, the nova was at a very high excitation phase at that time, and the intensities of the $[\text{N II}]$ lines were probably low.

If the last PBO measurement, $\log(\text{H}\alpha/\text{H}\beta) = 0.54$ is taken to be the final true value, then $E(B-V) = 0.24$ and $N_{21}(\text{H}) = 1.4$. We will take the extrapolated value of the Balmer decrement, leading to $E(B-V) = 0.19$, as the minimum likely reddening for the nova.

Paresce (1994) estimated the distance to the nova to be 3.5 ± 0.5 kpc on the basis of the proper motion and radial velocity of the expanding shell. At a distance of 3.5 kpc, $E(B-V) = 0.31$ implies a mean density of hydrogen of 0.17 cm^{-3} , a reasonable value for the gas along a spiral arm. The value $E(B-V) = 0.19$ implies a mean density of H of 0.10 cm^{-3} , which seems low.

The $E(B-V)$ from He II, 0.31, would require the $\log(\text{H}\alpha/\text{H}\beta) = 0.59$ after the shell becomes optically thin in the Balmer lines. The excess of 0.05 between this estimate and the last PBO value seems barely within the errors of the PBO measurement. Therefore, we think it unlikely that $E(B-V) > 0.31$. We will present models for assumed $N_{21}(\text{H})$ of 1.1 and 1.8, corresponding to $E(B-V) = 0.19$ and 0.31, respectively.

3.2. Sensitivity to Form of Carbon and H Column Density

We could fit the X-ray halo and the extinction law well with all materials and with all values of f_{vac} (the fraction of vacuum in the grains) if, and only if, we allow the value of $E(B-V)$ to be unreasonably small in order to optimize the fit. Compact grains (low f_{vac}) require optimum values of $E(B-V) \leq 0.02$, far below the actual value. We will discuss only values of $E(B-V) \geq 0.19$, in which case many models fail to explain the observations.

The type of carbon mixed with the silicates has a significant influence on the results. To fit the extinction, the carbon in grains must have a comparatively large imaginary part of the index of refraction (i.e., absorption) in the optical region, like that of the "BE" carbon in RM or the glassy carbon of Edoh. The "AC" carbon of RM is too transparent in this region of

the spectrum. The UV extinction is not a discriminant, since all forms of carbon have large absorption in that region. The hydrogen in the HAC carbons produces a band gap of 1–2 eV that drastically reduces the absorption in the optical region, so they produce the worst fits of all, with the more heavily hydrogenated material ("HAC9" of Alterovitz et al. 1991) significantly worse than "HAC5."

Composite grains with all forms of carbon have similar predictions for X-ray halos, so the halo tests the geometry of the grain and not the composition.

Figure 3 shows the extinction law results for models with $E(B-V) = 0.19$, along with the observations (triangles). The solid line is for grains with "BE" carbon, 50% vacuum; the dashed line is for compact "BE" grains. The short-dashed line shows HAC9 carbon, and the dot-dashed, "organic refractory," both with $f_{\text{vac}} = 0.5$.

The solid line in Figure 3 (the optical/UV extinction law) indicates that the RM "BE" AMC, with $f_{\text{vac}} = 0.5$ and $E(B-V) = 0.19$, produces a fairly good fit to the data. Its most discrepant extinctions are 9% low at $\lambda \approx 0.3 \mu\text{m}$ and $\approx 20\%$ too high for $\lambda < 0.15 \mu\text{m}$. The "AC" (not shown) and HAC9 do not provide enough extinction at V by 20% and are worse at $1 \mu\text{m}$. The organic refractory fit is very close to the "BE" for $\lambda < 0.4 \mu\text{m}$, but is too transparent in the visible. Compact "BE" grains produce only 76% of the required extinction at V . Edoh carbon (not shown) is very similar to "BE" for $1/\lambda < 5 \mu\text{m}^{-1}$, but its extinction has a pronounced dip on the short-wavelength side of the bump and drops to only 80% of the observations, lower than any other form of carbon. HAC5 is as low at V as organic refractory but has too much extinction at $6 \mu\text{m}^{-1}$, similar to HAC9.

Figure 4 is the same as Figure 3, but for $E(B-V) = 0.31$. Comparing Figure 3 and Figure 4, we see that increasing $E(B-V)$ to 0.31 makes the fit of the "BE" AMC, with $f_{\text{vac}} = 0.5$ somewhat worse, to being 12% too low at $3 \mu\text{m}$ and 30% too high at $1/\lambda = 7.6 \mu\text{m}^{-1}$. The extinction of the compact "BE" grains drops to 63% of the observed at V .

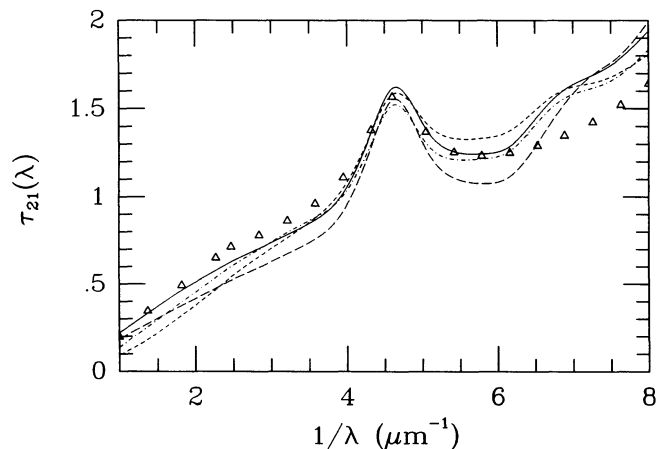


FIG. 3.—The extinction optical depth per 10^{21} H atoms, $\tau_{21}(\lambda)$, for various models, plotted against $1/\lambda$. All models were selected to produce the observed X-ray halo with $E(B-V) = 0.19$. Triangles, observations at the computed wavenumbers (Cardelli et al. 1989; O'Donnell 1994, with $R = 3.1$). Solid curve, grains including "BE" amorphous carbon (see Table 2), with f_{vac} (= fraction of vacuum) = 0.5; long dashes: "BE" amorphous carbon with compact grains ($f_{\text{vac}} = 0$); short dashes: grains with hydrogenated amorphous carbon "HAC9" carbon with $f_{\text{vac}} = 0.5$; dot-dashes: "Organic refractory" carbon, $f_{\text{vac}} = 0.5$.

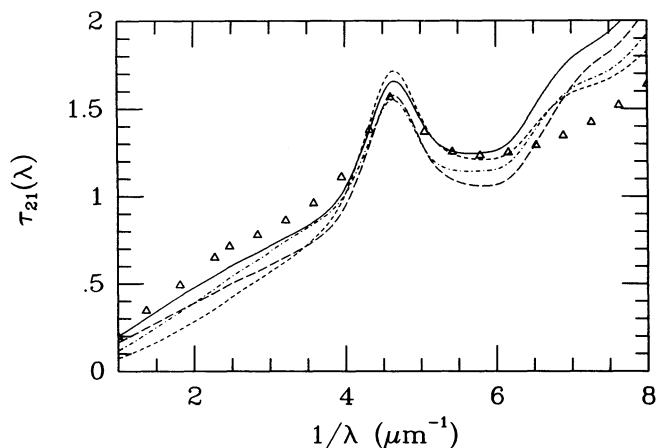


FIG. 4.—Same as for Fig. 3, assuming $E(B-V) = 0.31$

Figure 5 shows the X-ray halo observations (Table 1) and the calculated X-ray halos for $E(B-V) = 0.31$. The error bars are one standard deviation. A plot for $E(B-V) = 0.19$ would be almost the same and is not shown. In Figure 5 we see that “BE” carbon, with either f_{vac} shown (0 or 0.5), or others as well, fits the halo to within 2σ everywhere. The other carbons, especially HAC9, fail to fit the halo to within 2σ if we also require an attempt to fit the extinction law. Organic refractory fails to fit the slope of the halo by about 3σ . HAC5 has virtually identical X-ray properties to HAC9 and so fails to fit the halo.

Figure 6 shows the extinction of models with $E(B-V) = 0.31$, “BE” carbon, and $f_{\text{vac}} = 0, 0.25, 0.5$, and 0.8 , respectively, as the curves approach the observations in the optical/near-UV spectral region. All models fit the X-ray halo as well as that shown in Figure 5, but the extinction laws differ. The strongest conclusion is that compact grains fail to produce a satisfactory fit throughout the entire wavenumber range $1-3 \mu\text{m}^{-1}$, and also in the UV near $\approx 6 \mu\text{m}^{-1}$. At V the $f_{\text{vac}} = 0.25$ curve is somewhat below the $f_{\text{vac}} = 0.5$ and 0.8 values, but is similar at the shorter wavelengths. The $f_{\text{vac}} = 0.8$ fits the optical extinction law better than any other, but its improvement over

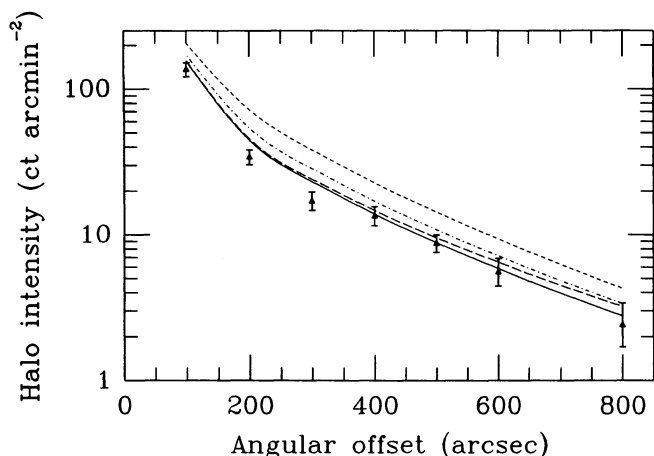


FIG. 5.—The shapes of the calculated X-ray halo for NC92 for the grain models whose extinctions are shown in Fig. 3, plotted against angular distance from the nova image. The observations are the points; the lines are as in Fig. 3. The error bars show 1σ . We see that “BE” carbon, either with $f_{\text{vac}} = 0$ or 0.5 , fits the observations within 2σ , while organic refractory and, especially, HAC9 carbons deviate more significantly.

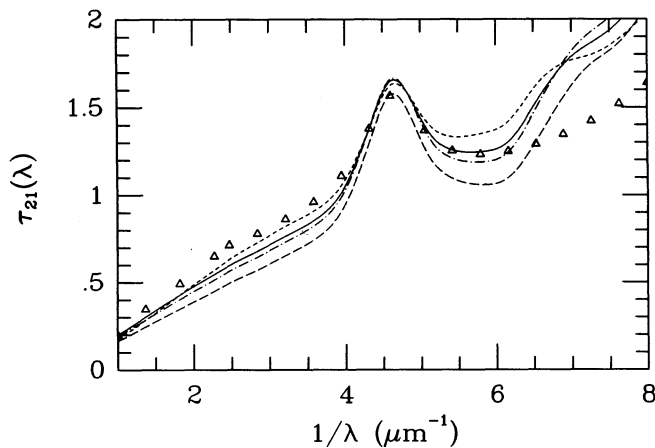


FIG. 6.—The fitting of the optical/ultraviolet extinction law for $E(B-V) = 0.31$ with “BE” amorphous carbon, with four amounts of vacuum included in the grains. Points: observations; long dashes: compact ($f_{\text{vac}} = 0$) grains; dot-dashes: $f_{\text{vac}} = 0.25$; solid line, $f_{\text{vac}} = 0.5$; short dashes, $f_{\text{vac}} = 0.80$.

$f_{\text{vac}} = 0.5$ is not large, and its deviations from the observations for wavenumbers greater than $5 \mu\text{m}^{-1}$ are worse than for 0.5 . Furthermore, the interstellar polarization suggests that $f_{\text{vac}} = 0.8$ is too much vacuum (see below).

3.3. Grain Size Distributions

Our models have a continuous distribution of sizes, arbitrarily confined to the range $0.005 \mu\text{m} \leq a \leq 3 \mu\text{m}$. The size distributions change with f_{vac} , as expected since the fluffy grains need to be larger to produce the same extinction. Figure 7 shows $a^4 n(a)$ plotted against a on a logarithmic scale, if $E(B-V) = 0.31$. The curve (if the ordinate were in linear units, not logarithmic) gives $dm(a)/d \ln a$, the differential mass contribution of grains in the size interval of width $d(\ln a)$. Each model in Figure 7 has the same total mass of grains. The MRN distribution is shown as the heavy solid line; the others all contain “BE” carbon with various parameters. The short dashes are for $p_- = -2$, $f_{\text{vac}} = 0.25$; the short/long dashes, for $f_{\text{vac}} = 0.8$. The solid and short-dashed lines are for $f_{\text{vac}} = 0.5$, with $p_- = 0$ and -2 , respectively. Note how much $p_- = -2$ reduces the

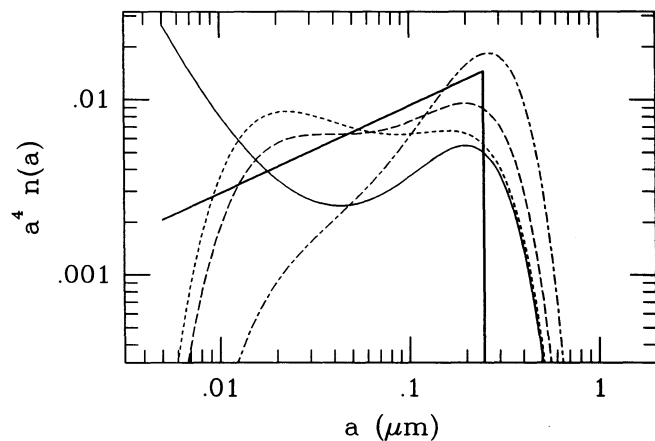


FIG. 7.—The mass distributions, $a^4 n(a)$, plotted against a for $E(B-V) = 0.31$, “BE” constants, all normalized to the same mass. The heavy solid line is the MRN distribution. Light solid line: $f_{\text{vac}} = 0.5$, $p_- = 0$. The others have $p_- = -2$. Short dashes, $f_{\text{vac}} = 0.25$; long dashes, $f_{\text{vac}} = 0.5$; short/long dashes, $f_{\text{vac}} = 0.8$.

numbers of smallest grains relative to the large. The amount of reduction is greater than one might think from inspecting equation (7), since the distribution is chosen to fit the extinction, and changes to any size range affect all other sizes. With $p_- = 0$, typically about 15% of the mass of grains is contained in sizes of $a \leq 0.007 \mu\text{m}$ but all of the available carbon is used by the model. If $p_- = -1$, the fit to the extinction law and halo is marginally better, only 1% of the mass is in grains with $a \leq 0.007 \mu\text{m}$, but about 15% of the carbon is not used by the model and could be in small grains. The models with more negative p_- have slightly more C and Si to provide the small grains that they do not include explicitly.

Kim, Martin, & Hendry (1994) fitted the $R = 3.1$ extinction law with a maximum entropy technique, using separate populations of compact silicate and graphite grains. Their derived mass distribution peaks near $a \approx 0.2 \mu\text{m}$ for silicates and $0.1 \mu\text{m}$ for graphite. For compact composite grains without the constraint of the halo, our size distribution peaks at $0.15 \mu\text{m}$, in between theirs. When we consider the halo, we need fluffy grains with sizes that are in the same range.

Thus, we cannot constrain the population of the smallest grains, but those of $a \approx 0.1\text{--}0.25 \mu\text{m}$ seem to need to be fluffy.

3.4. Sensitivity of Results to Other Parameters

Probably the major uncertainty in our results is the use of the Bruggeman effective medium theory to estimate the average index of refraction of the composite grain. The Maxwell-Garnett (MG) theory assumes that some materials ("impurities") are embedded in a matrix. If $f_{\text{vac}} \geq 0.5$, we took the carbon and silicates as impurities embedded in vacuum. Otherwise, silicate was the matrix. Models with the MG theory fit the extinction law less well than do those using the Bruggeman rule; the $\tau(V)$ for the best "BE" AMC models, with $f_{\text{vac}} = 0.5$ and $E(B-V) = 0.19$, decreased from 0.46 per 10^{21} H atoms using the Bruggeman rule to 0.42 with the MG theory, while the observed is 0.49. The differences between the rules became negligible in the UV part of the spectrum and for the X-ray halo. The fact that the two rules disagree on extinctions at most by 10% is encouraging but is no guarantee that either is correct. Some discrete dipole approximation calculations (e.g., Hage & Greenberg 1991; Ossenkopf 1991) suggest that the effective medium theories can give good approximations to the extinction of fluffy grains. However, the use of effective medium theory is especially dubious when the index of refraction becomes large, as is the case when the wavenumber becomes larger than $\approx 6 \mu\text{m}^{-1}$. We assume that the excess of extinction ($\approx 10\%$) we predict when $1/\lambda > 6 \mu\text{m}^{-1}$ might be caused by the failure of effective medium theory. Until the method of computing the actual extinction properties is improved, further "fine tuning" of the size distribution and composition beyond our simple approach does not seem warranted.

The fraction of vacuum in composite grains may well vary with grain size. We calculated some models in which f_{vac} is a linear function of a , either increasing or decreasing with size. Not surprisingly, the f_{vac} relevant to the sizes at the maximum of the contribution to the optical extinction and the halo, $\approx 0.2\text{--}0.3 \mu\text{m}$, determines the behavior of the model.

The geometry of the distribution of grains along the line of sight is not known, so we tried models with either the first or the last 30% of the path from us to the nova empty of grains. The results were very close to the uniform case. For $E(B-V) = 0.19$, the "BE" models predicted $\tau(V)$ per H drops from being 9% lower than the observed, for uniform $f(x)$, to

13% lower, and from 10% too high at $0.125 \mu\text{m}$ to 13% too high. It made almost no difference whether the grain-free gap was near the source or the observer.

Our assumption that the scattering is optically thin is good. The integrated strength of the halo out to $800''$, $2\pi \int I(\theta)\theta d\theta$, is 9600 ± 1500 counts. From the rate the halo strength is dropping with θ we estimate that the extension of the halo to large angles would add ≈ 1000 counts. The point source produced 6.6×10^4 counts, about 6 times the total halo, showing that the scattering is optically thin. Analysis of a thin halo, with single scattering, is far easier than multiple scattering.

4. DISCUSSION

Many diverse grain models fit the interstellar extinction law: composite grains (various materials mixed within the same grain), grains separately chemically homogeneous (such as MRN), or silicate cores with organic refractory mantles. An additional strong constraint on the size distribution is imposed by the X-ray halo.

Grains with small fraction of vacuum, f_{vac} , scatter X-rays too efficiently. Fluffy grains have less X-ray scattering efficiency for a given size, so the size distribution can accommodate large enough grains to produce the optical extinction without over-producing the X-ray halo. *We believe that the X-ray halo of NC92 provides significant evidence that grains are actually fluffy as opposed to being compact.* Our reservations about this statement arise mainly because of the approximations involving effective medium theories in calculating both the optical/UV extinction law and also for the X-ray scattering. Our result is in agreement with the X-ray halo of Cen X-3 (Woo et al. 1994), which also requires fluffy grains.

The present models are made with composite grains, with silicate, carbon, and vacuum within each grain. However, interstellar extinction and polarization can be fitted with separate populations of carbon and silicate grains (MRN; Draine & Lee 1984) or core/mantle grains (Greenberg 1989). The ability of these models to fit the extinction suggests that having the material combined within the same grain is not an essential feature of fitting the halo. It is the adding of vacuum that changes the X-ray scattering cross section relative to the optical extinction.

We are well aware of uncertainties in the composition of actual dust. Several possibilities include various oxides, sulfides, or other minerals, as well as other forms of carbon. However, the X-ray scattering of a grain depends very little upon its composition because the scattering is produced by all of the electrons of the various elements, including those in inner shells. These inner electrons will scatter independently of their arrangement within the solid, so compact grains with any chemical composition face the same general problem.

Our best models are not excellent fits to the optical extinction. As shown in Figures 3 and 4, the $f_{\text{vac}} = 0.5$ models fit better than $f_{\text{vac}} = 0$ but still need more absorption in the optical range and less for $1/\lambda > 6 \mu\text{m}^{-1}$. The fit is only marginally better for $f_{\text{vac}} = 0.8$ than for $f_{\text{vac}} = 0.5$, so other considerations are probably more important.

Interstellar polarization, another integral over the size distribution, is as much of a diagnostic of the alignment mechanism as of the size distribution of the grains. However, the wavelength dependence of the polarization, $p(\lambda)$, sets an upper limit on the amount of vacuum in the individual grains, because models show that $p(\lambda)$ does not fall rapidly enough toward small λ , even with perfect alignment, if grains have as

much as 80% vacuum (Wolff, Clayton, & Meade 1993). We assume that porosities with $f_{vac} \geq 0.8$ do not seem likely.

Duley (1994) showed that HAC produces an excellent fit to the profile of the $3.4 \mu\text{m}$ absorption feature seen in heavily reddened stars and suggests that HAC constitutes 20%–30% of the available carbon toward the Galactic center. HAC seems likely to be responsible for the “Extended Red Emission” seen in various objects (Witt 1989). However, the halo of NC92 suggests that neither HAC5 or HAC9, both with rather poor predictions for the halo, are the major carbonaceous component of grains. Our models show that interstellar carbon must produce more extinction in the optical/near-UV region than the laboratory samples of HAC. Perhaps the $3.4 \mu\text{m}$ absorption feature is produced in HAC that is more strongly absorbing in the optical region than HAC5.

Figure 7, giving the mass distribution of “BE” models, shows that all models have a mild hump or upturn in the mass distribution in the $a = 0.2\text{--}0.3 \mu\text{m}$ range. This is a property of every model that optimizes the fit to both the halo and extinction law, as well as MRN. Figure 7 also shows that neither the extinction law nor the X-ray halo are suitable diagnostics for very small grains. The light solid and dot-dashed lines are both $f_{vac} = 0.5$, but the latter has a small size cutoff ($p_- = -2$). It fits the data as well as the $p_- = 0$ model, but has little of its mass in small grains. It is clear that the NIR transient emission following the absorption of a single photon provides the best diagnostic for these small particles, unless significant studies of the extinction law at very short wavelengths become available.

Figure 8 shows the contribution per size interval to the extinction or to the X-ray halo at four wavelengths, relative to the maximum contribution per size interval. The grains have “BE” carbon, $f_{vac} = 0.5$, and the size distribution for the case $E(B-V) = 0.31$. The wavelengths are $1 \mu\text{m}$ (short dashes), V (long-short dashes), $0.153 \mu\text{m}$ (long dashes), and the halo at $100''$ (solid line), and $400''$ (dot-dashes). We see that the halo is produced by grains which are even larger ($\approx 0.25 \mu\text{m}$) than those producing the extinction at $1 \mu\text{m}$! The outer halo is produced by slightly smaller grains than the inner, but the effect is not large. As expected, the shorter wavelengths are produced by the smaller grains. We also see that even the UV extinction is produced by rather large grains ($\approx 0.08 \mu\text{m}$) with these fairly porous grains.

Figure 8 suggests why compact grains have trouble produc-

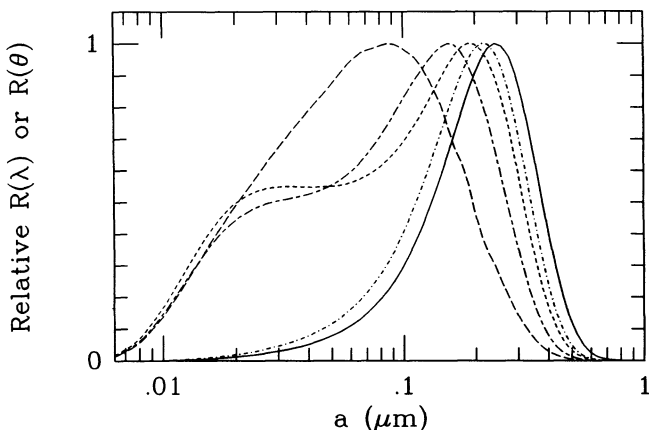


FIG. 8.—The contribution of grains of various sizes to the response for given extinctions and for X-rays, relative to the maximum contribution. All are for “BE” constants for carbon, $E(B-V) = 0.31$, $f_{vac} = 0.5$. Short dashes, $\tau(1 \mu\text{m})$; long-short dashes, $\tau(V)$; long dashes, $\tau(8 \mu\text{m}^{-1})$; solid, halo at $\theta = 100''$; dot-dashes, halo at $400''$.

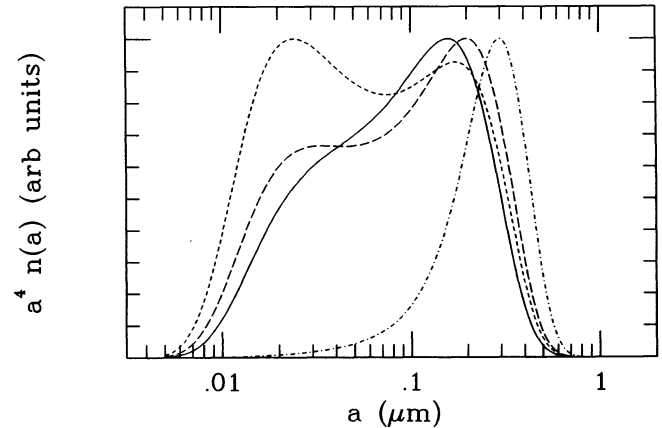


FIG. 9.—The mass distributions of the best fits for models of various f_{vac} , all for “BE” carbon, $E(B-V) = 0.31$, $p_- = -2$, relative to the maximum. Short dashes, $f_{vac} = 0$; long dashes, $f_{vac} = 0.25$; solid, $f_{vac} = 0.5$; dot-dashed, $f_{vac} = 0.8$. We see the shift in the size distribution as f_{vac} increases.

ing both the optical extinction per H and the halo. Grains in the size range $0.15\text{--}0.3 \mu\text{m}$ are the most effective in producing both optical extinction and the halo at all values of θ . The figure also shows that the UV extinction ($0.153 \mu\text{m}$; long dashes) is produced by grains of about $a = 0.09 \mu\text{m}$. This result is expected because the maximum of most extinction cross sections per mass occurs at $\lambda/2\pi \approx 4$, exactly as we find here since the mass distribution is not varying very fast in this size region (see Fig. 7).

Of course, the amount of the extinction per mass depends upon the optical constants. All of our derived extinctions are too large for $1/\lambda \geq 6.5 \mu\text{m}^{-1}$, with suggestions of a mild “bump” or spectral feature at $\approx 7 \mu\text{m}^{-1}$ (see Figs. 3, 4, or 6). This onset of strong absorption and the spectral feature are produced by the optical constants we used for the silicates (see Fig. 7 in Draine & Lee 1984) and would be present in any model using these constants. Two possibilities for explaining the conflict with observations are (a) the effective medium theories are wrong in dealing with large indices of refraction and overestimate the cross sections, and (b) some or most of the “silicates” are in fact metallic and silicon oxides, as is shown to be the case by depletions (Sofia et al. 1994).

Figure 9 shows the mass distribution, $a^4 n(a)$, plotted against $\log a$ for models with “BE” carbon, for the best fits to $E(B-V) = 0.31$, and with various values of f_{vac} , with the curves normalized to their maxima. As the grains become fluffy, the distributions shift from small to larger grains. The $f_{vac} = 0.8$ models (dot-dashed line) have most of the grain mass with $a > 0.2 \mu\text{m}$, while for $f_{vac} = 0$ (short dashes) the maximum occurs at $a = 0.02 \mu\text{m}$.

Scattering delays the arrival of X-rays as well as producing the halo (Trümper & Schönfelder 1973). The delay Δt for a photon arriving at an angle θ from the point source, after being scattered at fraction x along the path D from the observer, is

$$\Delta t = \theta^2 D x / [2c(1-x)]. \quad (9)$$

For $D = 3.5 \text{ kpc}$, $\theta = 200''$, and $x = 0.5$, Δt is only 2 days. The source intensity does not fluctuate on this timescale, so we do not have information from the timing of changes in the halo, as is possible for rapidly varying sources (Klose 1994).

This work has been partially supported by NASA grants NAGW-3833 and NAG 5-1683 to the University of Wisconsin. We appreciate thoughtful comments by Sumner Starrfield.

REFERENCES

- Alterovitz, A. S., Savvides, N., Smith, F. W., & Woollam, J. A. 1991, in *Handbook of Optical Constants of Solids II*, ed. E. D. Palik (New York: Academic), 837
- Barger, A. J., Gallagher, J. S., III, Bjorkman, K. S., Johansen, K. A., & Nordsieck, K. H. 1993, *ApJ*, 419, L85
- Bohlin, R. C., Savage, B. D., & Drake, J. F. 1978, *ApJ*, 224, 132
- Bohren, C. G., & Huffman, D. R. 1983, *Absorption and Scattering by Light in Small Particles* (New York: Wiley)
- Bussoletti, E., Colangeli, L., Borghesi, A., & Orofino, V. 1987, *A&AS*, 70, 257
- Cardelli, J. A., Clayton, G. C., & Mathis, J. S. 1989, *ApJ*, 345, 245
- Chochol, D., Hric, L., Urban, Z., Kromčík, J., & Papoušek, J. 1993, *A&A*, 277, 103
- Désert, F. X., Boulanger, F., & Puget, J. L. 1990, *A&A*, 237, 215
- Draine, B. T., & Anderson, N. 1985, *ApJ*, 292, 494
- Draine, B. T., & Lee, H. M. 1984, *ApJ*, 285, 89
- Duley, W. W. 1994, *ApJ*, 430, L133
- Greenberg, J. M. 1989, in *IAU Symp. 135, Interstellar Dust*, ed. L. J. Allamandola & A. G. G. M. Tielens (Dordrecht: Kluwer), 345
- Hage, J. I., & Greenberg, J. M. 1991, *ApJ*, 361, 251
- Hanner, M. 1988, in *Infrared Observations of Comets Halley and Wilson and Properties of Grains* (NASA Conf. Publ. 3004), 22
- Hasinger, G. 1994, *Rev. Modern Astron.*, in press
- Hauschildt, P. H., Starrfield, S., Austin, S., Wagner, R. M., Shore, S. N., & Sonneborn, G. 1994, *ApJ*, 422, 831
- Henke, B. L. 1981, in *Low-Energy X-Ray Diagnostics*, ed. D. T. Attwood & B. L. Henke (New York: AIP), 146
- Jenniskens, P. 1993, *A&A*, 274, 653
- Kim, S.-H., Martin, P. G., & Hendry, P. D. 1994, *ApJ*, 422, 164
- Klose, S. 1994, *A&A*, 289, L1
- Krautter, J., Ögelman, H., & Starrfield, S. 1992, *IAU Circ.*, No. 5550
- Krautter, J., Ögelman, H., Starrfield, S., Wichmann, R., & Trümper, J. 1994, in preparation
- Lacy, J. H., Knacke, R., Geballe, T. R., & Tokunaga, A. T. 1994, *ApJ*, 428, L69
- Martin, P. G. 1970, *MNRAS*, 149, 221
- Martin, P. G., & Rouleau, F. 1990, in *Extreme Ultraviolet Astronomy*, ed. R. F. Malina & S. Bowyer (Oxford: Pergamon), 341
- Mathis, J. S. 1990, *ARA&A*, 28, 37
- . 1993, *Rep. Prog. Phys.*, 56, 605
- Mathis, J. S., & Lee, C.-W. 1991, *ApJ*, 376, 490
- Mathis, J. S., Rumpl, W., & Nordsieck, K. H. 1977, *ApJ*, 217, 425 (MRN)
- Mathis, J. S., & Whiffen, G. 1989, *ApJ*, 341, 808
- Mauche, C. W., & Gorenstein, P. 1986, *ApJ*, 302, 371
- Morrison, R., & McCammon, D. 1983, *ApJ*, 270, 119
- O'Donnell, J. E. 1994, *ApJ*, 422, 158
- Ossenkopf, V. 1991, *A&A*, 251, 210
- Paresce, F. 1994, *A&A*, 282, L13
- Peimbert, M., Torres-Peimbert, S., & Dufour, R. J. 1994, *ApJ*, 418, 760
- Pfeffermann, E., et al. 1986, *Proc. SPIE*, 733, 519
- Puget, J.-L., & Léger, A. 1989, *ARA&A*, 27, 161
- Robbins, R. R. 1968, *ApJ*, 151, 511
- Rouleau, F., & Martin, P. G. 1991, *ApJ*, 377, 526 (RM)
- Savage, B. D., & Mathis, J. S. 1979, *ARA&A*, 17, 73
- Seaton, M. J. 1979, *MNRAS*, 187, 73P
- Shore, S. N., Sonneborn, G., Starrfield, S., Gonzalez-Riestra, R., & Ake, T. B. 1993, *AJ*, 106, 2408
- Shore, S. N., Sonneborn, G., Starrfield, S., Gonzalez-Riestra, R., & Polidan, R. S. 1994, *ApJ*, 421, 344
- Siebenmorgen, R., & Krügel, E. 1993, *A&A*, 259, 614
- Sofia, U. J., Cardelli, J. A., & Savage, B. D. 1994, *ApJ*, 430, 650
- Tielens, A. G. G. M., & Allamandola, L. J., ed. 1989, *IAU Symp. 135, Interstellar Dust* (Dordrecht: Kluwer)
- Trümper, J., & Schönfelder, V. 1973, *A&A*, 25, 445
- Witt, A. N. 1989, in *IAU Symp. 135, Interstellar Dust*, ed. L. J. Allamandola & A. G. G. M. Tielens (Dordrecht: Kluwer), 367
- Witt, A. N., Stecher, T. P., Boroson, T. A., & Bohlin, R. C. 1989, *ApJ*, 336, L21
- Wolff, M. J., Clayton, G. C., & Meade, M. R. 1993, *ApJ*, 403, 722
- Woo, J. W., Clark, G. W., Day, C. S. R., Nagase, F., & Takeshima, T. 1994, *ApJ*, 436, L5